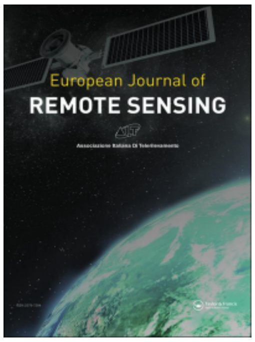

European Journal of Remote Sensing

ISSN: 2279-7254 (Online) Journal homepage: www.tandfonline.com/journals/tejr20

Functional ecosystem properties estimated from satellite PRISMA and Sentinel-2 data in natural European sites

Gaia Vaglio Laurin, Lorenza Nardella, Alessandro Montaghi, Alessandro Sebastiani, Bartolomeo Ventura, Alessandro Mei, Carlo Calfapietra & Dario Papale

To cite this article: Gaia Vaglio Laurin, Lorenza Nardella, Alessandro Montaghi, Alessandro Sebastiani, Bartolomeo Ventura, Alessandro Mei, Carlo Calfapietra & Dario Papale (2026) Functional ecosystem properties estimated from satellite PRISMA and Sentinel-2 data in natural European sites, European Journal of Remote Sensing, 59:1, 2669420, DOI: 10.1080/22797254.2026.2669420

To link to this article: https://doi.org/10.1080/22797254.2026.2669420

Published online: 08 May 2026.

EUROPEAN JOURNAL OF REMOTE SENSING
2026, VOL. 59, NO. 1, 2669420
https://doi.org/10.1080/22797254.2026.2669420

Taylor & Francis by informa

RESEARCH ARTICLE

OPEN ACCESS Check for updates

Functional ecosystem properties estimated from satellite PRISMA and Sentinel-2 data in natural European sites

Gaia Vaglio Laurin[a], Lorenza Nardella[b], Alessandro Montaghi[c,d], Alessandro Sebastiani[e], Bartolomeo Ventura[f], Alessandro Mei[g], Carlo Calfapietra[b] and Dario Papale[a]

[a]Research Institute off Terrestrial Ecosystems (IRET), National Research Council (CNR), Montelibretti, Italy; [b]Research Institute on Terrestrial Ecosystems (IRET), National Research Council (CNR), Porano, Italy; [c]Research Institute on Terrestrial Ecosystems (IRET), National Research Council (CNR), Sesto Fiorentino, Italy; [d]Institute for BioEconomy (IBE), National Research Council (CNR), Sesto Fiorentino, Italy; [e]Department for Sustainability, Circularity and Climate Adaptation (SSPT), Italian National Agency for New Technologies, Energy and Sustainable Economic Development (ENEA), Rome, Italy; [f]Eurac Research, Institute for Earth Observation, Bolzano, South Tyrol, Italy; [g]Institute on Atmospheric Pollution Research (IIA), National Research Council (CNR), Montelibretti Research Area, Rome, Italy

ABSTRACT

Science-based indicators are needed to monitor ecosystems at different scales, especially with increasing climate change and anthropogenic pressures, and varying impacts according to the scale of analysis. Ecosystem functional properties report on key ecosystem processes and dynamics at multiple scales, from community to biome level, providing a dynamic view of ecosystem carbon- and energy-related processes, useful for monitoring short-term changes. These quantities can be derived from flux measurements, such as those collected by the Integrated Carbon Observation System flux tower network. Here, modeling of selected ecosystem functional properties with hyperspectral satellite data was carried out at fifteen European sites belonging to five different plant functional types. The results, compared to those obtained using a dense Sentinel-2 time series, highlight the potential of hyperspectral narrowbands. Gross primary productivity, light use efficiency and net ecosystem exchange have been predicted with reasonable accuracy, independently by the plant functional type or site latitude . Two different modeling approaches have been compared: Random Forests and Extreme Gradient Boosting. The potential of monitoring ecosystems using the EFPs approach is discussed in consideration of the pros and cons in data use, and the future increased availability of hyperspectral missions.

ARTICLE HISTORY
Received 6 December 2025
Revised 30 March 2026
Accepted 30 April 2026

KEYWORDS
PRISMA; Sentinel 2; ecosystem functional properties; ICOS; GPP; LUE

Introduction

Climate change continues to negatively impact natural resources and biodiversity, and the pressure on terrestrial land is increasing together with world population growth. Multiple and combined climate and anthropogenic impacts affect terrestrial resources: to mitigate losses in natural resources and their diversity, robust science-based indicators are needed. Indicators that can inform on vegetation dynamics and functions, such as the processes of photosynthesis and respiration, water loss, nutrient uptake, or radiation interception, are especially relevant for the sustainable management of resources and the provision of ecosystem services.

In the last decade, multiple studies have focused on understanding plant and ecosystem functions under climate change, anthropic disturbance impacts and extreme event scenarios. Among them, innovative approaches include those based on eddy covariance (EC) flux measurements (Baldocchi, 2020). Various functional indicators have been employed in different contexts: such as in the case of functional indicators of biodiversity that were linked to disturbance response at the community-level (Mouillot et al., 2013); or the functional traits in the global leaf economic spectrum (LES), whose changes have been employed to

CONTACT Dr. Gaia Vaglio Laurin gaia.vagliolaurin@cnr.it Research Institute offTerrestrial Ecosystems (IRET), National Research Council (CNR), Montelibretti Research Area Rome 1, Italy
Supplemental data for this article can be accessed online at https://doi.org/10.1080/22797254.2026.2669420.

detect vegetation changes and dynamics, as they are usually linearly related to climate factors at the biome scale (Wright et al., 2004; 2017). When using functional traits, the community level is especially important for understanding adaptations to anthropogenic and climate-related impacts. In fact, trait values at fine spatial grain may differ substantially even under similar climate and soil conditions, as they are mainly filtered by disturbances, fine-scale soil conditions, niche partitioning and biotic interactions (Bruelheide et al., 2018). However, LES plant traits might lack sensitivity at this community level, showing clearer variations at the biome scale (Gillison, 2019).

Ecosystem functional properties (EFPs), or "quantities that characterize ecosystem processes and responses in an integrated and comparable manner" (Reichstein et al., 2014), have demonstrated their ability to report ecosystem processes and dynamics at multiple scales – from the community to the biome level- and in different ecosystems (Baldocchi, 2020; Musavi et al., 2016; Vaglio Laurin et al., 2020), thus representing an advantage.

EFPs inform the process of carbon uptake in vegetation, describing ecosystem efficiency in the use of water and light; they are dependent on community and ecosystem traits and structure and environmental drivers and are influenced by land use and climate change. Key processes are captured by EFPs, such as photosynthesis, respiration and evapotranspiration, together with their relationship with resource use, providing a dynamic view of ecosystem carbon- and energy-related processes that is useful for monitoring short-term changes (Keenan et al., 2013; Musavi et al., 2015).

The Integrated Carbon Observation System (ICOS) network, a landmark of the European Strategy Forum on Research Infrastructures (ESFRI), collects long-term observations of gas and energy exchanges between ecosystems and the atmosphere at more than 100 terrestrial stations in Europe, covering different ecosystems such as various forest types, grasslands, wetlands, croplands, peatlands etc. At ICOS sites, EC instrumentation usually sets up on a tower, measures continuously the net fluxes of greenhouse gases, water and energy between ecosystems and the atmosphere, as well as all the major living and nonliving components and drivers controlling or affecting flux exchanges. ICOS is one of the flux networks that measure and process data consistently (e.g. AmeriFlux, NEON, OzFlux, AsiaFlux, etc.) that all together constitute the FLUXNET global network, providing crucial data and information to better understand ecosystem functions from flux observation integrated across time and space.

The EFPs are derived from flux measurements after standardization, processing and quality control by the ICOS Ecosystem Thematic Centre (Pastorello et al., 2020; Vitale et al., 2020); EFPs include the light use efficiency (LUE), or the capacity of vegetation to convert the incoming light into fixed carbon; the water use efficiency (WUE), or the ability to convert each unit of water loss by evapotranspiration in gross biomass production, as photosynthetic rate is directly related to water loss in transpiration through plant stomata; Bowen ratio (BW), or the ratio of energy used for warming in comparison with the one used for evapotranspiration, that is higher in bare and dry soils; the gross primary production (GPP), or the photosynthetic capacity of the ecosystem; and net ecosystem exchange (NEE), or the overall carbon dioxide exchange between a terrestrial ecosystem and the atmosphere, taking into account both photosynthesis and respiration.

Linking remote sensing observations with measures of ecosystem processes and dynamics is fundamental to upscale sparse field data over larger areas and over time, allowing an effective monitoring of natural resources and their changes. At the regional and global levels, EFPs have been upscaled using remote sensing, meteorological data and machine learning (Jung et al., 2011; Tramontana et al., 2016). At the ecosystem and local levels, multispectral data such as Sentinel-2 (S2) time series data have been used to map regional ecosystem functional types, intended as patches of land surface showing similarities in carbon dynamics Liu et al. 2020), and the role of S2 in inferring plant functional diversity from space has also been documented (Ma et al., 2019), together with its capability to monitoring functional traits during a severe drought (Savinelli et al., 2024). Hyperspectral (HS) data, characterized by the acquisition of continuous and contiguous narrowband wavelengths, in contrast with the subset of broadband wavelengths used in multispectral data, bring a higher information content and are increasingly recognized as key to understanding and predicting the adaptation of ecosystems to environmental changes (Zhang et al., 2021). For example, HS remote sensing allows the detection of the functional signatures of vegetation in heat landscapes, enabling distinctions among different plant strategies (Schmidt et al., 2017), the retrieval of leaf traits and their links to ecosystem productivity in grasslands (Zhao et al., 2021), and the characterization of floodplain meadow biodiversity within a plant functional trait framework (Punalekar

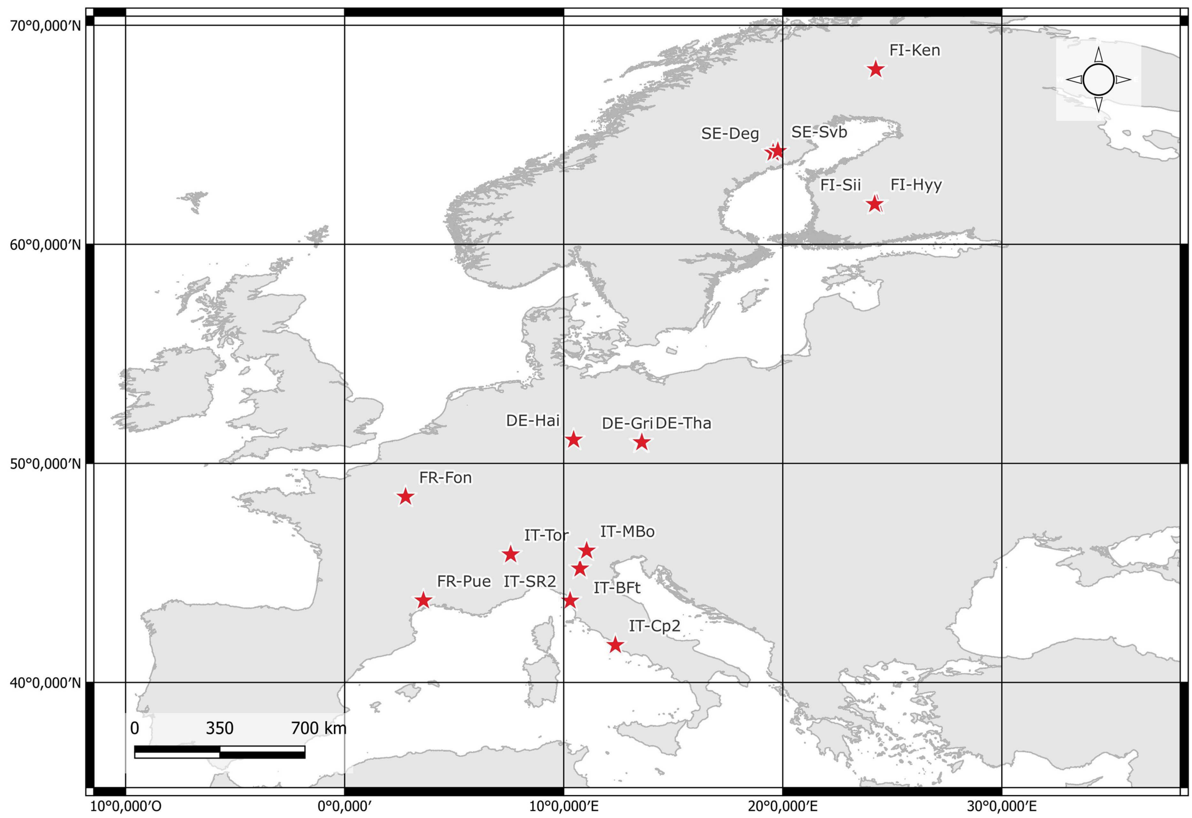

Figure 1. Location of the 15 study sites (ICOS field stations) in Europe.

et al., 2016). Such previous research, having an ecosystem functional approach, has usually been carried out with airborne or Hyperion satellite data. Now, the mapping of vegetation functions is entering a new era, with two ongoing satellite missions and others in the advanced preparatory phase, such as the European Space Agency (ESA) Copernicus Hyperspectral Imaging Mission for the Environment (CHIME) and the National Aeronautics and Space Administration (NASA) Surface Biology and Geology (SBG) mission. Among the ongoing HS satellite missions, there are the Environmental Mapping and Analysis Program (EnMAP) of the German Space Agency (DLR) and the Hyperspectral Precursor of the Application Mission (PRISMA) of the Italian Space Agency (ASI), which share very similar features. Specifically, PRISMA is equipped with a hyperspectral sensor that collects 240 bands from the visible to the shortwave infrared regions at 30 m spatial resolution (Cogliati et al., 2021), being well suited to perform analyses at the community and ecosystem scale.

Recently, vegetation traits (leaf chlorophyll, nitrogen and water contents, leaf mass area and leaf area index) retrievals based on PRISMA data were investigated in forests (Micol et al., 2024) and crops (Tagliabue et al., 2022), and the correlation between PRISMA data and EFPs was investigated in selected European natural ecosystems (Vaglio Laurin et al., 2024).

Here, the objective is to test the retrieval of EFPs with PRISMA time series at 15 ICOS stations, with vegetation belonging to five different plant functional types (PFT), and sites located in five European countries. The results are discussed in comparison with those obtained using a dense Sentinel-2 time series, which argues for the potential of the EFPs approach in consideration of the future increased availability of HS missions.

Methods

Study sites and EFPs data

The present study covers homogeneous sites surrounding 15 ICOS flux tower stations in five European countries (Figure 1), where PRISMA cloud-free images in the March to October 2020–2023 active vegetation period were available. The 15 sites belong to five plant functional types (PFT), listed in Table 1, which also shows the number of available PRISMA images per site and data reference. Additional information on the vegetation characteristics at each site is found in Table SM1 in Supplementary materials (SM).

Flux Level 2 data were downloaded from the ICOS Carbon Portal (https://data.icos-cp.eu/portal/), which provides half-hourly eddy covariance fluxes, including gross primary productivity (GPP), net ecosystem exchange (NEE), sensible heat (H), incoming shortwave radiation (SW) and latent heat (LE). GPP and NEE are both measures of carbon fluxes and ecosystem productivity; while the former represents gross carbon uptake due to photosynthetic activity and is indicative of biomass production potential within the ecosystem, the latter is a measure of net carbon flux and defines whether an ecosystem acts as a carbon sink or a carbon source, also informing the climate change mitigation potential of the ecosystem (Pei et al., 2022; Urban et al., 2007). SW refers to the quantity of solar radiation in the short wave region of the electromagnetic spectrum that is largely correlated with the photosynthetically active radiation available to the vegetation at Earth's surface. LE and H represent two forms of heat transfer, the former occurring with a phase change and no change in temperature, the latter only with a temperature change, both playing key roles in atmospheric processes and energy exchange relevant for EC measurements (Oke, 1987).

Flux data were selected from dates coincident with those of PRISMA acquisitions; the half-hourly fluxes from 9:30 to 11:00 (usual time for PRISMA pass over the sites) were averaged on a daily basis.

Three EFPs were computed according to Vaglio Laurin et al. (2020), namely: water use efficiency (WUE = GPP/LE), light use efficiency (LUE = GPP/SW) and Bowen ratio (BW = H/LE), while GPP and NEE were included in the original datasets. The WUE and LUE measure how effectively plants convert water and incoming SW into biomass through photosynthesis (Monteith, 1972; Stanhill, 1986); BW describes heat transfer, reflecting ecosystem water availability (Wilson et al., 2002). For those few cases in which the required input variables were not available, gap-filled values provided by the ICOS dataset were used (Vekuri et al., 2023). The gap-filling technique is optimal at mid-latitudes but might introduce errors at very high latitudes (>60°), a fact taken into account for the FI-Ken site (68° latitude). Outliers in EFPs (1 for WUE and 2 for BW) were removed using the interquartile range method: they were reviewed case by case in order: (a) to retain those bringing relevant information with a sound ecological base and (b) exclude those due to systematic ICOS flux tower artifacts. In the former case, observations were replaced by median values while in the latter, they were excluded by the dataset, reason why GPP, NEE and LUE each had 70 observations, whereas the WUE and BW had 69 and 68 observations, respectively. The total number of samples per site and PFT is reported in Table 1.

Table 1. Study sites: name, plant functional type (PFT), number of available PRISMA images and reference for flux data to the data object that ensure reproducibility as requested by the data license.

Site	PFT	PRISMA	Reference
FI-Ken	ENF	4	Laurila et al. (2025)
FI-Hyy	ENF	2	Mammarella et al. (2025)
FI-Sii	WET	2	Tuittila et al. (2025)
FR-Fon	DBF	6	Berveiller et al. (2025)
FR-Pue	EBF	7	Limousin et al. (2025)
DE-Gri	GRA	5	Bernhofer et al. (2025a)
DE-Hai	DBF	4	Knohl and Tiedemann (2024)
DE-Tha	ENF	5	Bernhofer et al. (2025b)
IT-BFt	DBF	4	Gerosa et al. (2025)
IT-Cp2	EBF	10	Fares et al. (2025)
IT-MBo	GRA	4	Gianelle et al. (2025)
IT-SR2	ENF	7	Arriga et al. (2025)
IT-Tor	GRA	3	Cremonese et al. (2025)
SE-Deg	WET	4	Nilsson et al. (2025)
SE-Svb	ENF	3	Peichl et al. (2025)

Abbreviations: EBF = evergreen broadleaf forest (2 sites); ENF = evergreen needleleaf forest (5 sites); DBF = deciduous broadleaf forest (3 sites); GRA = grassland (3 sites) and WET = wetland (2 sites).

Remote sensing data

Seventy PRISMA 2A atmospherically and radiometrically corrected products were downloaded from the Italian Space Agency portal (https://prisma.asi.it). Each product includes 240 bands, with 66 in the visible to near infrared region (VNIR), 173 in the shortwave infrared region (SWIR), plus 1 panchromatic (PAN). A preliminary data inspection revealed 3 missing bands (237 in total) and several corrupted ones (stripes, strong noise) that were excluded, reducing the number to 192. Specifically, the excluded bands were: 1 to 9, 104 to 111, 148 to 164 and 227 to 234. For additional noise removal, the minimum noise fraction transformation (MNF; Green et al., 1988) was applied, including: (a) a forward transformation based on the eigenvalues of the noise covariance matrix, using bands with eigenvalues < 10; (b) an inverse transformation using the spectral subset in (a). Very few pixels having negative values were set to 0; then, PRISMA images were clipped using a 90 m circular buffer around the ICOS tower locations, with this buffer set to collect a statistically representative number of pixels. By definition, the flux towers are set in homogeneous areas, however vegetation homogeneity was further checked against the 2018 Corine land cover level IV dataset to ensure cover by a single class, and computing the coefficient of variation (CoV) of the normalized difference vegetation index (NDVI) for the PRISMA pixels included the buffer. Setting a threshold of NDVI CoV < 10%, all the sites exhibited homogeneous vegetation in the buffer and a single land cover class. The PRISMA pixels falling inside the buffer for at least 70% of their area were extracted and used in subsequent tests. 111 vegetation indices (VIs) describing multiple vegetation characteristics (e.g. chlorophyll, water content, dry matter, pigments, structure, carotenoids, senescence, nitrogen, lignin and cellulose) were computed per each image according to the "Prismaread" R package (Busetto & Ranghetti, 2020); the original 128 indices included in the package were screened to correct for few errors in the formulas, with few indices excluded due to previous band removal here performed in the preprocessing step. Those VIs values out of the interquartile range were removed as outliers after the absence of an ecological meaning was evaluated and were replaced by median values according to Hron et al. (2010). The median was preferred to the mean because it is a more robust statistic (50% breakdown point), providing a stable representation of the typical signal at each pixel. Overall, for PRISMA, 542 values across all VI observations were identified as outliers based on the IQR, approximately equal to 7% of the whole dataset. For Sentinel-2, the total number is 48 values, about 2.4% of the whole dataset.

Sixty-seven Sentinel-2 Level-2A (S2 L2A) atmospherically corrected images covering the study sites were acquired on dates as close as possible to the PRISMA images; the number of days from/before the PRISMA dates was in the range 0-42, with only four images acquired more than ±7 days with respect to PRISMA. Using Google Earth Engine (GEE) (Mutanga & Kumar, 2019), each S2 L2A image was filtered using the scene classification layer (SCL) to keep valid clear-sky pixels. The images were used to compute 30 VIs according to the S2 Toolbox in the SentiNel Application Platform (SNAP) of the European Space Agency. The VIs were computed using the average of pixels falling for at least 70% into a 90 m-radius circular buffer around each flux tower; outlier values were removed using the interquartile range approach after excluding the occurrence of any ecological meaning for those values and were replaced by median values according to Hron et al. (2010). The S2-related elaborations were performed in Google Earth Engine, while outliers' removal was carried out using RStudio (version 4.2.2).

One of the objectives of this research is to comparatively test PRISMA and Sentinel 2 based models, with input flux data always extracted from the exact date of the available image for each dataset. The PRISMA and S2 acquisition plans are however different, meaning that in few cases models refer to slightly different periods of the season, which could have an impact on the sensors comparison. Therefore, the temporal offset between the PRISMA and S2 data was analyzed; the mismatch was 4 days in 92.5% of the cases, and no relevant vegetation change can be safely assumed. Then, in three cases, the temporal mismatch was in the 7–15 days range, and only in two cases in the 24–42 days range, with the latter implying moving from early to late spring. This occurred in an evergreen broadleaf forest characterized by minimal intraseasonal phenological changes and in a mire habitat with continuous growth throughout the spring. As the large majority of relationships (92.5%) are built in comparable periods and flux data is always temporal coincident with satellite data, it is reasonable to conclude that modeling relationships on slightly different dates does not impact the robustness of the EFP-VIs relationships, also considering that any change in vegetation status is reflected in both the flux and the reflectance information.

Data analysis

The VIs computed from PRISMA and Sentinel-2 images were used as inputs into random forest (RF) and extreme gradient boosting (XGBoost) models to predict the EFPs derived at ICOS flux tower sites. The results of the models based on RF and XGBoost were compared, as well as those based on PRISMA or S2 data.

Random forest is a well-established ensemble machine learning method that is built on the foundation of decision trees and improves it through bagging and random feature selection, which allows for the decorrelation of trees and decreases model variance (Breiman, 2001). Differently from RF, already largely adopted in vegetation remote sensing, the XGBoost algorithm has scarcely been tested in this context or for ecosystem functional modelling, and therefore its characteristics are illustrated here in more detail. The choice of comparing these two approaches derives from their different features, as summarized in Table 2.

Gradient boosting is a nonparametric machine learning technique introduced by Friedman (2001) and Friedman (2002), which was originally designed to fit nonparametric generic predictive models using gradient descent in feature space. The boosting idea is to combine base learners (weak learners that are slightly better than random) into a strong learner in an iterative way (Yoav et al., 1999). In gradient tree boosting, many base weak learners are built sequentially from the pseudo-residuals, which corresponds to the gradient of the loss function of the previous tree. In each iteration, a tree is constructed from a random subsample of the dataset, chosen without replacement, resulting in incremental improvement in the model (Moisen et al., 2006). Chen and Guestrin (2016) proposed an efficient, scalable implementation of the gradient tree boosting framework called extreme gradient boosting (XGBoost), a decision-tree-based ensemble method that builds classification or regression trees one by one, with the residuals of the previous tree used to train the subsequent model to achieve a better outcome (Zhang et al., 2023). Several algorithmic optimizations characterize XGBoost performance, controlling the complexity of the model and reducing overfitting; furthermore, it has appropriate approaches to reduce computational complexity and increase training speed. The algorithm requires a thorough hyper-parameter tuning with a large number of hyperparameters to set (Lima Marinho et al., 2024).

Optuna is a popular optimization framework (Akiba et al., 2019; Fu et al., 2023) that has three specific features: (i) a define-by-run context; (ii) an efficient sampling and pruning mechanism; and (iii) ease of configuration. The (i) define-by-run criteria allows the user to dynamically construct the search space, which in XGBoost is formed by multiplying the values of all the hyperparameters selected for optimization; different hyperparameter combinations are evaluated to minimize a given function, i.e. loss function, and the function score is the output of the search; the hyperparameters are dynamically generated and statistically sampled based on the history of previously evaluated trials. For sampling (ii), Optuna includes

Table 2. Summary of the main features of RF and XGBoost machine learning approaches.

	Random forest	Extreme gradient boosting
Year introduced	2001 (by Breiman, L.)	2016 (by Chen, T. and Guestrin, C.)
Task	Classification and regression	Classification and regression
Algorithm type	Decision tree ensemble via bagging	Decision tree ensemble via gradient boosting
Base method	Fully grown decision trees (high variance, low bias)	Shallow decision trees (boosted sequentially)
Learning paradigm	Bagging (parallel trees)	Boosting (sequential tree correction)
Variance handling	Strong	Moderate
Bias handling	Limited	Strong
Handling missing values	Not handled natively	Handled natively
Tuning	Not strictly necessary (robust with default settings)	Necessary for optimal performance
Tuning complexity	Low	High
N. of main hyperparameters	4–5	8–12
Regularization	Implicit (via bagging and tree constraints)	Explicit (L1, L2 and structural penalties)
Feature sampling	yes	yes
Overfitting risk	Low to moderate	Higher if not regularized properly
Overfitting control	Tree depth, minimum samples per split/leaf	Tree depth, learning rate, L1/L2 penalties, gamma
Sensitivity to noise	Lower (due to averaging)	Higher (requires tuning to prevent overfitting
Variable importance	Available	Available
Training speed	Faster (parallelizable)	Slower (sequential training), but optimized for speed
GPU support	Limited	Native GPU support
Distribution	R, Python, C++, Java	R, Python, C++, Java
Use case	High variance datasets	High-bias datasets and complex relationships
Overall performance	Strong baseline	Often state-of-the-art with tuning

various independent algorithms; with the tree-structured Parzen estimator (TPE) algorithm (Bergstra et al., 2011) here used; for (ii) efficient pruning or strategies for the termination of unpromising trials, here the default Optuna pruner was adopted, called Median Pruner. For (iii) ease of configuration, Optuna is fully integrated in Python (from version 3.8), allowing easy setup and use for a variety of tasks (Akiba et al., 2019). In Supplementary materials, the full list of hyperparameters optimized using the Optuna framework is presented in Table SM2.

Models set up in RF and XGBoost

To avoid inflating random forest models due to the multicollinearity of VIs inputs, a feature selection step was initially performed in "VSURF" (variable selection using random forests; Genuer et al., 2019) R package, similarly to Parisi et al. (2024). A two-step strategy was adopted: (i) features are ranked based on the variable importance (VarImp) score averaged over 50 runs, with a few retained based on a threshold established by a CART model; (ii) a collection of nested RF models is built, progressively adding the retained features as inputs. The final feature selection is based on the model yielding the smallest out-of-bag (OOB) error averaged over 25 runs.

Subsequently and for each EFP, a random forest model was run using the features selected in the previous step, using the R package "caret" (Kuhn, 2008), where *mtry*, *ntree* and *nodesize* parameters were tuned (Probst et al., 2019). *Mtry* controls the number of features (p) considered at each split; its default value is $p/3$ and here the tuning was tested from 1 to p. *Ntree* sets the total number of trees in the forest; its default value is 500, and here values equal to 500 and 1000 were tested. *Nodesize* sets the minimum number of samples required to split a node; its default value is 5, and the tuning range here was set from 1 to 10. The model's performance was evaluated through 5- and 10-fold cross validation (5 CV; 10 CV), reporting the best result. The coefficient of determination (R^2) and the root mean squared error (RMSE) were used as accuracy metrics. Hyper-parameterization was similarly performed for models based on PRISMA and S2 data.

The XGBoost models, fitted using the XGBoost package (version 2.1.3), received as input features the same VIs selected by VSURF. The model hyper parametrization was carried out in Optuna (v. 4.1.0; Table SM2 in Supplementary materials for parameter meaning and adopted values); different cross-validation approaches were performed (Leave-One-Out, 10-fold and 5-fold) and the results were evaluated using R^2 and RMSE accuracy values. All the modeling steps were carried out in Python (version 3.12).

Results

Random forests models based on PRISMA data were characterized by high to moderate accuracy for 4 out of 5 EFPs, namely, GPP, NEE, LUE and BW, with R^2 values ranging from 0.71 to 0.37. The model for WUE was unsuccessful ($R^2 = 0.03$). The RF models run after tuning the *ntree*, *mtry* and *nodesize* parameters always provided an increase in accuracy with respect to the default values used in the preliminary runs (Table 3). 10CV provided higher validated accuracy in all cases, but one (BW). Details on the selected indices and their importance in the model, according to the results of variable importance analysis, are presented in Supplementary materials (SM; Table SM3, Figure SM1). The random forests EFPs models based on Sentinel-2 data (SM; Table SM4) for all flux sites obtained lower accuracy than those based on PRISMA VIs in most cases (Table 3), and the prediction of WUE was unsuccessful too ($R^2 = 0.03$). For the other EFPs the R^2 values ranged from 0.65 (GPP) to 0.5 (BW).

The PRISMA narrowband indices contribute differently to the models, bringing information from various spectral regions. According to variable importance (Figure SM1 in Supplementary materials), the main contributions came: for GPP from VOG2 and MTCI; for NEE from VOG2 and OSAVI2; for LUE from VOG2, VOG1 and DWSI2; and for BW from the Gitelson2 and MCARI/OSAVI indices. The VOG indices, so often selected, are based on red edge narrow hyperspectral bands, sensitive to the foliage chlorophyll concentration, canopy leaf area and water content (Vogelmann 1993), with the MTCI being a surrogate of the red edge index (Dash & Curran, 2004). The OSAVI indices (Wu et al., 2008) are modified versions of the Soil Adjusted Vegetation Index (Huete, 1988): exploiting the NIR and red spectrum but accounting for the soil background. The DWSI indices report about water stress (Apan et al., 2004),

Table 3. Tuned PRISMA and Sentinel-2 random forest models providing higher accuracy, with information on selected vegetation indices (VIs) (other details for VIs in Supplementary materials; SM, Tables SM3 and SM4), parametrization values (*ntree, mtry, nodesize*), cross validation (CV) approach, R^2 and RMSE values.

PRISMA random forest models					
	GPP	NEE	LUE	WUE	BW
VIs	VOG2, MTCI, OSAVI2, LWVI2, MTVI2, DWSI1, MSI, CRI4, CI, TVI	OSAVI2, VOG2	VOG2, VOG1, DWSI2	Datt5, Datt8, CRI3	MCARI/OSAVI, Gitelson2
ntree	500	1000	1000	500	500
mtry	7	1	3	2	2
nodesize	4	10	9	9	4
CV method	10CV	10CV	10CV	10CV	5CV
R^2	0.71	0.61	0.62	0.03	0.37
RMSE	3.64	3.38	0.01	0.05	1.63
Sentinel-2 random forest models					
	GPP	NEE	LUE	WUE	BW
VIs	S2REP, IRECI	IRECI, REIP, MTCI, S2REP, ARVI	ARVI, RVI, IRECI, NDTI, MNDVI, NDPI	GEMI, NDVI	BI, BI2, MNDVI
ntree	500	500	500	500	1000
mtry	1	3	2	2	1
nodesize	3	7	9	8	6
CV method	10CV	5CV	10CV	5CV	5CV
R^2	0.65	0.55	0.58	0.03	0.5
RMSE	4.2	3.86	0.01	0.08	1.36

exploiting the shortwave infrared region. The Gitelson2 index (Gitelson et al., 2003) informs on chlorophyll and photosynthetic activity through the red edge and infrared regions; while the MCARI/OSAVI is a chlorophyll absorption index (MCARI), which is based on the near infrared and sensitive to leaf area index, modified to account for the soil background (Daughtry et al., 2000). In summary, information from the red, infrared and especially the red edge region is critical in all cases, with only the LUE model exploiting the shortwave region. In Sentinel-2 based models, the red and infrared broadbands and the red-edge narrowband resulted all useful, with the LUE model also exploiting the SWIR region similarly to what is found in PRISMA based models. In summary, the types of indices and spectral regions resulted very similar in both the PRISMA or Sentinel-2 models.

Below, the scatterplots between the predicted and observed values for the best PRISMA random forest GPP, NEE, LUE and BW models (Figure 2) are shown; different symbols indicate latitudinal partitioning (High, Mid, Low latitudes) with no visible clustering effects; similarly, different colors indicate different PFT (as in Figure SM2 in SM), with no clustering occurrence.

To better assess the influence of plant functional types in the models, a RF test using PRISMA data was performed with only data from the three forest types, corresponding to a reduced subset of 10 flux sites and 53 PRISMA scenes. Results are slightly less accurate than those obtained using data from all sites, except for BW, and are as follows: GPP ($R^2 = 0.64$, RMSE = 3.95), NEE ($R^2 = 0.52$, RMSE = 3.59), LUE ($R^2 = 0.53$, RMSE = 0.01), WUE ($R^2 = 0.04$, RMSE = 0.05) and BW ($R^2 = 0.43$, RMSE = 1.64).

In addition, to further investigate the capacity of the models to capture a general EFP response to VIs across different PFTs, and given the limited number of observations for certain PFTs (WET in particular, with only 6), we tested mixed-effect models (MEMs) for each EFP separately, using PRISMA predictors selected by VSURF (Table 3). MEMs includes both fixed and random effects, with fixed effects setting a multiple regression, and random effects allowing regression parameters (intercept or/and slope) to vary across groups or clusters (here PFTs), capturing group-specific deviations from the overall trend. Models were built with the R package “lme4” (v.4.5.1). The MEMs results are reported in Table SM5 in Supplementary materials. The results indicate that the variance of random effects given by PFTs was equal to zero for NEE, LUE and WUE, thus absent. For GPP, random intercept effects were negligible, with intraclass correlation coefficient (ICC = random_effect_variance/total_variance) equal to 0.05. For BW ICC scored 0.19, suggesting possible but minimal group differences; therefore for BW, the intercept and slope were tested together, obtaining an ICC of 0.52 and a conditional R^2 of 0.57, with respect to the 0.5 of the RF model. Given this limited increase in only one case and considering that the BW MEM model is based on a numerically limited sample, we concluded that PFT impacts have not or minimal influence, but additional tests with larger sample size are needed to confirm it. The extreme gradient boosting (XGBoost) algorithm is gaining popularity for being optimized for speed and performance: it was here tested with the

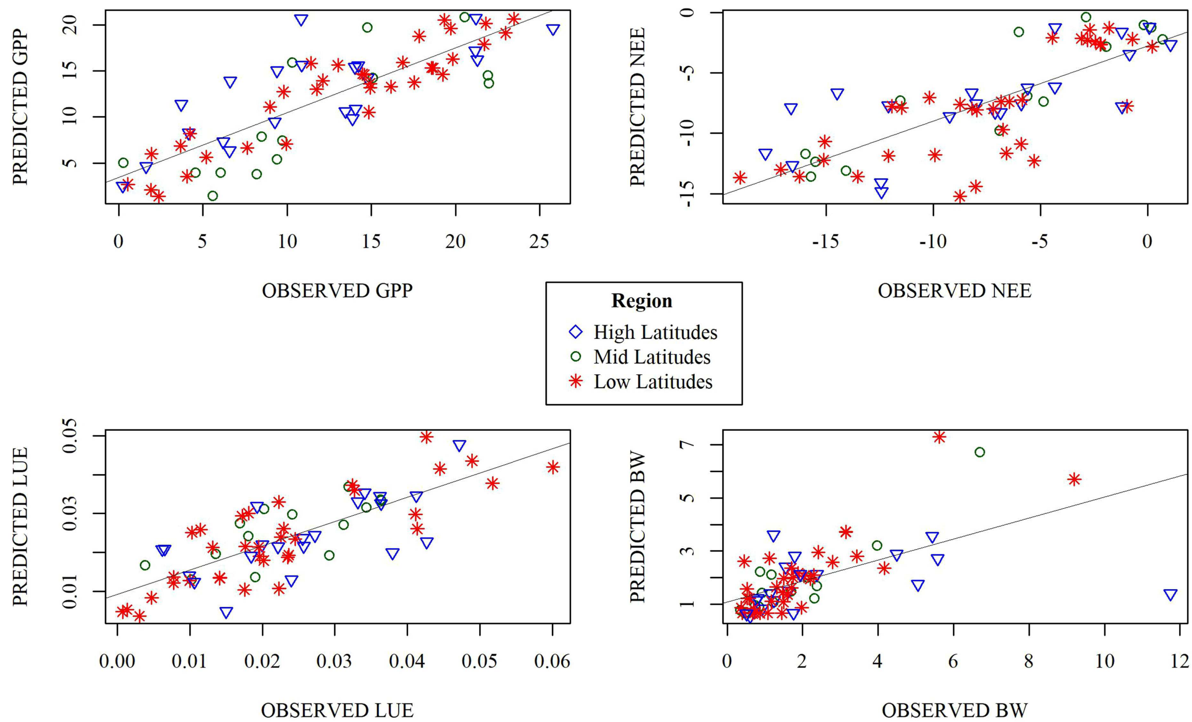

Figure 2. Scatterplots of predicted vs observed EFPs values for GPP, NEE, LUE and BW obtained with tuned random forests models, using selected vegetation indices as inputs and with cross validation. The WUE scatterplot was not included for unsuccessful retrieval ($R^2 = 0.04$). Latitude ranges are represented by different symbols and colors.

Table 4. XGBoost best models accuracy (R^2, RMSE) per EFP using the selected PRISMA VI inputs reported in Table 3 and LOO validation approach.

	GPP	NEE	LUE	WUE	BW
Booster option	Dart	Dart	GBtrees	Dart	GBtrees
R2	0.72	0.63	0.68	−0.13	0.22
RMSE	3.56	0.008	0.007	0.05	1.8

purpose of comparison with random forests, and with the same PRISMA input features (VIs, in Table 3) of the most accurate RF model. Both the DART and the gbtree booster options were tested, adopting different cross-validation approaches. The XGBoost results are comparable when using different cross validation approaches. Here only those obtained with LOO are included in Table 4, having slightly better accuracy; the corresponding parameterization values are reported in Table SM2 in SM. The full set of results obtained with other cross-validation approaches not reported in the main text of the manuscript (RF on PRISMA, RF on S2, XGB on PRISMA) are available in Table SM6 in Supplementary materials.

XGBoost models obtained high to moderate accuracy for 3 out of 5 EFPs (0.72–0.63R^2 range), with values similar to those obtained with random forests models. Models for WUE and BW were unsuccessful (WUE $R^2 = -0.13$; BW $R^2 = 0.22$); the best improvement in accuracy is observed for LUE ($R^2 = 0.68$), that with RF model resulted having a R^2 value equal to 0.62.

Discussion

The functioning of ecosystems is governed by carbon, water, energy and nutrients biogeochemical processes, occurring simultaneously in multiple biotic and abiotic system compartments (Schulze et al., 2019). Ecosystem functions can be quantified in several ways, one of which is the calculation of ecosystem functional properties from eddy covariance measurements Migliavacca et al 2021), an approach that integrates different processes, such as carbon allocation and partitioning, organic matter decomposition and nutrient cycles, as well as plant functional traits and meteorological variability. Upscaling this ground information is critical to model ecosystem dynamics in the face of a changing climate. Hyperspectral data is clearly important in this context, given its large amount of information content and the increased number of missions expected shortly (Zhang et al., 2021). Here, a set of EFPs obtained from 15 European sites and belonging to 5 PFT were predicted by PRISMA data. The results show that monitoring ecosystem processes through space is, in most cases, feasible and provides an integrated approach to monitor ecosystem dynamics.

Insights from data analysis

The tuned EFPs models ingest information of different plant functional types, including three forest types (deciduous and evergreen broadleaf and evergreen needleleaf), grasslands and wetlands, producing accurate predictions for most of the considered functional variables. When testing only forest sites, the results were only slightly less accurate even if the low number of samples imposed caution in interpretation; these results obtained with a data subset indicate good performance even in a restricted range of ecosystem processes, such as those characterizing the forest. This preliminary study suggests that EFPs retrieval with hyperspectral data is robust for key variables that can be estimated in regions with mixed or multiple ecosystems; however, the independence of the models from specific life types and thus model broad applicability shall be further tested. The idea is however supported by the study of Pacheco-Labrador et al. (2017), who predicted GPP in a tree-grass ecosystem with relative errors of ~36% using airborne high-resolution hyperspectral data, evidencing that at the footprint scale, the ecosystem signals are quite homogeneous despite tree and grass mixture. The reported scatterplots suggest the absence of a latitude or PFT influence in this study. Unfortunately, tests on single PFT other than forests were not possible due to limited data availability: a larger dataset with more samples from different sites and PFTs needs to be evaluated to confirm or exclude any influence in models. A larger dataset would also allow the testing of potential differences in the seasonal relationships between fluxes and optical measurements, which were observed by Nestola et al. (2016) for LUE in grasslands, where a slight change in efficiency between the first and second halves of the growing season occurred.

Reasonably accurate results were obtained for GPP, NEE and LUE, and moderate results for BW; instead, the retrieval of WUE was unsuccessful, and additional research is needed to clarify this outcome. Gomarasca et al. (2024) also reported weak WUE models based on Sentinel-2 spectral data. The WUE was previously retrieved using VOD from microwave satellite data (Vaglio Laurin et al., 2020), but -differently from multi and hyperspectral data, the VOD-water relationship is well rooted in theoretical and empirical evidence (Holtzman et al., 2021).

Previous studies relating the WUE with spectral indices found positive relations in mono-specific crops, where the GPP and evapotranspiration are easily controlled. In natural ecosystems, the different occurring species can adopt very different strategies for water management, potentially generating noise in the relationship between ecosystem evapotranspiration (here, simulated by latent heat to derive WUE) and the spectral signal, a reason that could justify the weaker WUE–VIs links. For instance, in the presence of drought, *Quercus ilex* reduces stomatal conductance, with decreased evapotranspiration but unchanged canopy reflectance (Manes et al., 2006), while *Fagus sylvatica* having limited drought tolerance, shows a rapid decrease in evapotranspiration and an immediate reduction in photosynthesis and canopy reflectance (Borišev et al., 2024). Furthermore, WUE is here derived from GPP and latent heat: GPP alone has a good relationship with VIs, suggesting LE-specific noisy dynamics or uncertainty in this flux measure. Other ways to compute WUE are available, e.g. exploiting evapotranspiration values, and additional research could be done in this direction, as well as in understanding the role of different water use strategies where a mix of species is present.

The results based on Sentinel-2 are in most cases, less accurate than those based on PRISMA, supporting the idea that at the habitat or ecosystem level the narrowband information from hyperspectral data is more important than the higher spatial resolution of multispectral data, as already observed in Zabeo et al. (2024). The results show an agreement between the two sensors with respect to the spectral regions that are more important in modeling: the red, infrared and especially red-edge portion being are selected because of their links with photosynthetic activity. The short-wave infrared region is relevant for LUE retrieval, with the exploited bands (around 1660 and 2100 nm) located in correspondence to peaks of reflectance by biochemical components. In these regions, lignins and other phenolic and polyphenolic compounds acting as defense, antioxidants and sunscreens in leaves are known to influence leaf optical properties (Li et al., 2023).

In terms of algorithms, XGBoost models produced slightly higher accuracies than the RF, but at the higher cost of fine tuning of several hyperparameters. Fine tuning requests specific expertise, which is not always available when thinking about a broad application context. In our view, the accuracy improvement brought by XGBoost is useful but not so high to justify the replacement of the RF, which is well diffuse and has a manageable modeling framework.

Advantages and limitations of PRISMA and EFPs

The availability of tools for VIs computation, as well as for performing feature selection, now makes the management of dozens of hyperspectral bands easier. Hyperspectral data can generate an impressive number of indices, and these tools improve the capability to work with such complex data, also leaving room for research aimed at testing new indices and bands combinations. In this sense, future research plans to investigate the spectral indices selection per plant functional type, also exploiting data from fixed radiometers installed at flux tower sites, similarly to what was illustrated by Nestola et al. (2018).

PRISMA data are known to be affected by some issues that have to be addressed before data use. An example is the geolocation inaccuracy, with the need to co-register the images over other datasets (e.g. S2). Issues in obtaining on-demand data due to the many requests are also known, as well as noise occurring in different spectral regions that imposes spectral resampling to exclude corrupted bands (Vaglio Laurin, 2025; Zabeo et al., 2024). While PRISMA shows mode accurate EFPs predictions with respect to multispectral data, the S2 imagery availability is significantly better, and S2 represents a fundamental data source in certain regions. Further research could consider the integration of these two data types.

Flux measurements are a crucial source of ecosystem information, and the continuous availability of new measurements from the ICOS and other research infrastructures is essential. However, uncertainty sources, in particular in the GPP estimation (Pastorello et al., 2020), the potential spatial heterogeneity of the site (in terms of ecosystem functions and responses), and the variability of the footprint (the area monitored by the eddy covariance system), are important issues to consider. Further studies are needed to provide ground data able to additionally validate the EFPs quantities derived from flux data at different locations.

While a quantitative evaluation of the uncertainty related to this methodology is not possible at this time, some considerations can still be derived. The semi-hourly ICOS flux measurements are characterized by random uncertainty, footprint variability and sensors biases. In the first case, averaging the measures in a 2-hour time period and performing outliers exclusion is the way here adopted here to minimize this source of uncertainty; with respect to spatial footprint variability, the selection of an ecologically homogeneous area around the tower, instead of the exact footprint to extract remote sensing data, is expected to reduce the impact of this source; finally, the careful review of data quality by the ICOS Ecosystem Thematic Center, as well as the active management of the sites, is expected to minimize sensors failure or the inclusion of artifacts in the data. In urban and vegetated areas, previous studies based on two towers established that the uncertainty of sensible and latent it is below 8% (Järvi et al., 2018). In this study, the PRISMA-S2 comparison is potentially affected by the temporal mismatch between the sensors: data analysis shows that 62 out of the 67 PRISMA-S2 pairs (92.5%) are characterized by a very limited temporal mismatch (max. 4 days), which is unlikely to represent important changes in vegetation development. Furthermore, the extracted fluxes correspond to the satellite date, meaning that any vegetation change should be reflected in fluxes changes.

To further understand the hyperspectral-EFPs links, future research shall be performed broadening the sample size, target changes in EFPs following disturbance and extreme events, and adopting other less tested EFPs. These properties could also be integrated into metrics of multifunctionality that can be better linked to biodiversity. Waiting for the forthcoming HS missions, it is important to keep investigating the links between space and ground information, which is critical for improving ecosystems understanding and monitoring.

Conclusions

Previous research based on flux data demonstrated that carbon-related fluxes are relevant for ecosystem models (Chang et al., 2021): the EFPs conveniently resume multiple ecosystem functions and represent a valuable approach at different scales. This approach has various advantages: the prediction of EFPs based on hyperspectral data has been preliminarily tested in other researches (Vaglio Laurin et al., 2024; Pacheco-Labrador et al., 2017, and Pacheco-Labrador et al., 2020), showing the potential to study ecosystem functioning with an innovative and integrated look. EFPs can also contribute to climate change research, as demonstrated by Vaglio Laurin et al. (2020), who detected with vegetation optical depth (VOD) large anomalies in forest GPP and LUE after extreme climate events. EFPs might also be useful in biodiversity research too; in fact biodiversity is one of the main drivers of ecosystem functioning, enhancing the productivity and stability of communities also in relation to extreme events (Mahecha et al., 2022). EFPs computed at 44 sites of the National Ecological Observatory Network (Thorpe et al., 2016) were predicted using Sentinel 2 spectral data, climate and vegetation structure information, and resulted to be clearly influenced by arboreal biodiversity (Gomarasca et al., 2024). Satellite hyperspectral data can strongly contribute to clarifying the biodiversity-ecosystem functioning relationship (BEF) by exploiting the spectral-EFPs-biodiversity link.

Overall, this research represents a further step to understand how to exploit innovative space-based information for integrated ecosystem monitoring via the EFP approach, contributing to produce valuable information for better monitoring our natural resources in an era of climate change and increased anthropogenic impacts.

Acknowledegments

GVL and DP acknowledge the PNRR, Missione 4, Componente 2, Avviso 3264/2021, IR0000032—ITINERIS—Italian Integrated Environmental Research Infrastructures System CUP B53C22002150006. LN acknowledges the project PRIN 2020 “MULTIFOR—Multi-scale observations to predict Forest response to pollution and climate change_PRIN_2020_LS9”. The authors thank all the data providers from ICOS and declare that they have no conflict of interest.

Author contributions

CRediT: **Gaia Vaglio Laurin:** Conceptualization, Methodology, Supervision, Writing – original draft, Writing – review & editing; **Lorenza Nardella:** Formal analysis, Investigation; **Alessandro Montaghi:** Formal analysis; **Alessandro Sebastiani:** Conceptualization, Formal analysis, Writing – review & editing; **Bartolomeo Ventura:** Formal analysis; **Alessandro Mei:** Methodology; **Carlo Calfapietra:** Supervision; **Dario Papale:** Data curation, Supervision.

Disclosure statement

No potential conflict of interest was reported by the author(s).

Funding

No funding was received.

ORCID

Gaia Vaglio Laurin 0000-0002-6728-3557
Lorenza Nardella 0000-0002-2383-0643
Alessandro Montaghi 0000-0001-8351-0230
Alessandro Sebastiani 0000-0003-4877-3769
Bartolomeo Ventura 0000-0002-8898-4205
Alessandro Mei 0000-0002-5665-5917
Carlo Calfapietra 0009-0006-6220-887X
Dario Papale 0000-0001-5170-8648

Data availability statement

The data that support the findings of this study are available in the Zenodo repository at 10.5281/zenodo.17762649.

Vaglio Laurin (2025). Functional ecosystem properties estimated from satellite PRISMA and Sentinel-2 data at natural European sites [Data set]. Zenodo. https://doi.org/10.5281/zenodo.17762649

The data were derived from the following resources available in the public domain: PRISMA ASI (https://prismauserregistration.asi.it/); Sentinel-2 Copernicus (https://dataspace.copernicus.eu/explore-data) and ICOS flux data (https://www.icos-cp.eu/data-services/about-data-portal).

References

Akiba, T., Sano, S., Yanase, T., Ohta, T., & Koyama, M. (2019). Optuna: A next-generation hyperparameter optimization framework. *In Proceedings of the 25th ACM SIGKDD international conference on knowledge discovery & data mining*. 2623–2631.

Apan, A., Held, A., Phinn, S., & Markley, J. (2004). Detecting sugarcane 'Orange rust' disease using EO-1 hyperion hyperspectral imagery. *International journal of remote sensing*, *25*(2), 489–498. https://doi.org/10.1080/01431160310001618031

Arriga, N., Goded, I., Dell'Acqua, A., & Matteucci, M. (2025). ETC L2 ARCHIVE from san rossore 2, 2019–2024. *ICOS RI*. https://hdl.handle.net/11676/Mfe9bdiDJuMVXW7tIBJuJXMc

Baldocchi, D. D. (2020). How eddy covariance flux measurements have contributed to our understanding of global change biology. *Global change biology*, *26*(1), 242–260. https://doi.org/10.1111/gcb.14807

Bergstra, J., Bardenet, R., Bengio, Y., & Kégl, B. (2011). Algorithms for hyper-parameter optimization. *Advances in neural information processing systems*, *24*

Bernhofer, C., Eichelmann, U., Grünwald, T., Hehn, M., Mauder, M., Moderow, U., & Prasse, H. (2025a). ETC L2 ARCHIVE from Grillenburg, 2017–2024. *ICOS RI*. https://hdl.handle.net/11676/u9fOOmV_hphObRN9rSRyTJgH

Bernhofer, C., Eichelmann, U., Grünwald, T., Hehn, M., Mauder, M., Moderow, U., & Prasse, H. (2025b). ETC L2 ARCHIVE from tharandt, 2020–2024. *ICOS RI*. https://hdl.handle.net/11676/4SDuyFmHhz7R1HlM2Mi9GsqN

Berveiller, D., Dufrêne, E., Delpierre, N., Morfin, A., Vincent, G., Bazot, S., Soudani, K., Girardin, C., Guillot, T., & Perot-Guillaume, C. (2025). ETC L2 ARCHIVE from Fontainebleau-Barbeau, 2019–2024. *ICOS RI*. https://hdl.handle.net/11676/z6OPRwwsjIG1rk5_HlkuQXb8

Borišev, M., Župunski, M., Arsenov, D., Nikolić, N., Tarčak, S., & Pajević, S. (2024). Understanding beech (Fagus sylvatica L.) photosynthetic responses to microhabitat water deficit: A site-specific investigation. *European Journal of Forest Research*, *143*(6), 1611–1625. https://doi.org/10.1007/s10342-024-01702-z

Breiman, L. (2001). Random forests. *Machine Learning*, *45*, 5–32. https://doi.org/10.1023/A:1010933404324

Bruelheide, H., Dengler, J., Purschke, O., Lenoir, J., Jiménez-Alfaro, B., Hennekens, S. M., Jandt, U., Botta-Dukát, Z., Chytrý, M., Field, R., Jansen, F., Kattge, J., Pillar, V. D., Schrodt, F., Mahecha, M. D., Peet, R. K., Sandel, B., van Bodegom, P., Altman, J., … Wirth, C. (2018). Global trait–environment relationships of plant communities. *Nature ecology & evolution*, *2*(12), 1906–1917. https://doi.org/10.1038/s41559-018-0699-8

Busetto, L., & Ranghetti, L. (2020). A tool for facilitating access and analysis of PRISMA L1/L2 hyperspectral imagery v1.0.0, URL: https://doi.org/10.5281/zenodo.4019081. https://irea-cnr-mi.github.io/prismaread/

Chang, S. C., Saitoh, T. M., Shibata, H., & Suzuki, S. N. (2021). Recent advances in the understanding of ecosystem processes at eddy covariance CO2 flux sites in east asian forest ecosystems: A review. *Journal of Agricultural Meteorology*, *77*(1), 52–65. https://doi.org/10.2480/agrmet.D-20-00018

Chen, T., & Guestrin, C. (2016). Xgboost: A scalable tree boosting system. *In Proceedings of the 22nd acm sigkdd international conference on knowledge discovery and data mining*, 785–794. https://doi.org/10.1145/2939672.2939785

Cogliati, S., Sarti, F., Chiarantini, L., Cosi, M., Lorusso, R., Lopinto, E., Colombo, R., Miglietta, F., Genesio, L., Guanter, L., Damm, A., Pérez-López, S., Scheffler, D., Tagliabue, G., Panigada, C., Rascher, U., Dowling, T., & Giardino, C. (2021). The PRISMA4 imaging spectroscopy mission: Overview and first performance analysis. *Remote sensing of environment*, *262*. 112499. https://doi.org/10.1016/j.rse.2021.112499

Cremonese, E., Galvagno, M., & Morra di Cella, U. (2025). ETC L2 ARCHIVE from Torgnon, 2016–2024. *ICOS RI*. https://hdl.handle.net/11676/JZIDLUbkyXeyHCypLm6JIaPu

Dash, J., & Curran, P. J. (2004). Evaluation of the MERIS terrestrial chlorophyll index, *IGARSS 2004. 2004 IEEE International Geoscience and Remote Sensing Symposium* (Vol. *1*). IEEE.

Daughtry, C. S., Walthall, C. L., Kim, M. S., De Colstoun, E. B., & Iii, McMurtrey, J. E. (2000). Estimating corn leaf chlorophyll concentration from leaf and canopy reflectance. *Remote sensing of Environment*, *74*(2), 229–239.

Fares, S., Alivernini, A., Chianucci, F., Conte, A., Corsanici, R., Ilardi, F., Moretti, V., & Sorgi, T. (2025). ETC L2 ARCHIVE from Castelporziano2, 2021–2024. *ICOS RI*. https://hdl.handle.net/11676/qmciSgs5YEENoaTDzm-Zdr9S

Friedman, J. H. (2001). Greedy function approximation: A gradient boosting machine. *Annals of statistics*, *29*, 1189–1232. https://doi.org/10.1214/aos/1013203451

Friedman, J. H. (2002). Stochastic gradient boosting. *Computational statistics & data analysis*, *38*(4), 367–378. https://doi.org/10.1016/S0167-9473(01)00065-2

Fu, B., Liang, Y., Lao, Z., Sun, X., Li, S., He, H., Sun, W., & Fan, D. (2023). Quantifying scattering characteristics of mangrove species from optuna-based optimal machine learning classification using multi-scale feature selection and Sar image time series. *International Journal of Applied Earth Observation and Geoinformation*, *122*. 103446. https://doi.org/10.1016/j.jag.2023.103446

Genuer, R., Poggi, J. M., Tuleau-Malot, C., & Genuer, M. R. (2019). Package 'vsurf'. *Pattern Recognition Letters*, *31*(14), 2225–2236.

Gerosa, G., Bignotti, L., Finco, A., Marzuoli, R., & Plebani, D. (2025). ETC L2 ARCHIVE from Bosco Fontana, 2019–2024. *ICOS RI*. https://hdl.handle.net/11676/LPXD6kqUgB3hQdSDwQuzanBD

Gianelle, D., Belelli Marchesini, L., Cavagna, M., Marcolla, B., Rodeghiero, M., Vescovo, L., & Zampedri, R. (2025). ETC L2 ARCHIVE from Monte Bondone, 2022-01-01–2024-01-08. *ICOS RI* https://hdl.handle.net/11676/2URn417sWYN0ROUJMIXjCiTq0101202408.

Gillison, A. N. (2019). Plant functional indicators of vegetation response to climate change, past present and future: II. Modal plant functional types as response indicators for present and future climates. *Flora*, *254*, 31–58. https://doi.org/10.1016/j.flora.2019.04.001

Gitelson, A. A., Gritz, Y., & Merzlyak, M. N. (2003). Relationships between leaf chlorophyll content and spectral reflectance and algorithms for non-destructive chlorophyll assessment in higher plant leaves. *Journal of plant physiology*, *160*(3), 271–282. https://doi.org/10.1078/0176-1617-00887

Gomarasca, U., Duveiller, G., Pacheco-Labrador, J., Ceccherini, G., Cescatti, A., Girardello, M., … Migliavacca, M. (2024). Satellite remote sensing reveals the footprint of biodiversity on multiple ecosystem functions across the NEON eddy covariance network. *Environmental Research: Ecology*, *3*(4), 045003.

Green, A. A., Berman, M., Switzer, P., & Craig, M. D. (1988). A transformation for ordering multispectral data in terms of image quality with implications for noise removal. *in IEEE Transactions on Geoscience and Remote Sensing*, *26*(1), 65–74. https://doi.org/10.1109/36.3001

Holtzman, N. M., Anderegg, L. D., Kraatz, S., Mavrovic, A., Sonnentag, O., Pappas, C., Konings, A. G., Cosh, M. H., Langlois, A., Lakhankar, T., Tesser, D., Steiner, N., Colliander, A., & Roy, A. (2021). L-band vegetation optical depth as an indicator of plant water potential in a temperate deciduous forest stand. *Biogeosciences*, *18*(2), 739–753. https://doi.org/10.5194/bg-18-739-2021

Hron, K., Templ, M., & Filzmoser, P. (2010). Imputation of missing values for compositional data using classical and robust methods. *Computational Statistics & Data Analysis*, *54*(12), 3095–3107. https://doi.org/10.1016/j.csda.2009.11.023

Huete, A. R. (1988). A soil-adjusted vegetation index (SAVI). *Remote sensing of environment*, *25*(3), 295–309. https://doi.org/10.1016/0034-4257(88)90106-X

Järvi, L., Rannik, Ü., Kokkonen, T. V., Kurppa, M., Karppinen, A., Kouznetsov, R. D., Wood, C. R., Rantala, P., & Vesala, T. (2018). Uncertainty of eddy covariance flux measurements over an urban area based on two towers. *Atmospheric Measurement Techniques*, *11*(10), 5421–5438. https://doi.org/10.5194/amt-11-5421-2018

Jung, M., Reichstein, M., Margolis, H. A., Cescatti, A., Richardson, A. D., Arain, M. A., Williams, C., Arneth, A., Bernhofer, C., Bonal, D., Chen, J., Gianelle, D., Gobron, N., Kiely, G., Kutsch, W., Lasslop, G., Law, B. E., Lindroth, A., Merbold, L., … Vaccari, F. (2011). Global patterns of land atmosphere fluxes of carbon dioxide, latent heat, and sensible heat derived from eddy covariance, satellite, and meteorological observations. *Journal of Geophysical Research: Biogeosciences*, *116*(G3), G001566. https://doi.org/10.1029/2010JG001566

Keenan, T., Hollinger, D. Y., Bohrer, G., Dragoni, D., Munger, J. W., Schimd, H. P., & Richardson, A. D. (2013). Increase in forest water-use efficiency as atmospheric carbon dioxide concentrations rise. *Nature*, *499*(7458), 324–327. https://doi.org/10.1038/nature12291

Knohl, A., Tiedemann, F., Klosterhalfen, A., Markwitz, C., & Siebicke, L. (2024). ETC L2 ARCHIVE from Hainich, 2018-12-31–2023-12-31. *ICOS RI* https://hdl.handle.net/11676/HraNB_GeItn8UdBmcpeZBfV4.

Kuhn, M. (2008). Building predictive models in R using the caret package. *Journal of Statistical Software*, *28*(5), 1–26. https://doi.org/10.18637/jss.v028.i05

Laurila, T., Aaltonen, H., Aurela, M., Hatakka, J., Rainne, J., Suopajärvi, S., & Varjonen, S. (2025). ETC L2 ARCHIVE from Kenttarova, 2020–2024. *ICOS RI*. https://hdl.handle.net/11676/gSdgMtAhq0u-yL7espMVIlan

Li, C., Czyż, E. A., Halitschke, R., Baldwin, I. T., Schaepman, M. E., & Schuman, M. C. (2023). Evaluating potential of leaf reflectance spectra to monitor plant genetic variation. *Plant Methods*, *19*(1. 108. https://doi.org/10.1186/s13007-023-01089-9

Lima Marinho, T., do Nascimento, D. C., & Pimentel, B. A. (2024). Optimization on selecting XGBoost hyperparameters using meta-learning. *Expert Systems*, *41*(9), e13611. https://doi.org/10.1111/exsy.13611

Liu, R., Huang, F., Ren, Y., Wang, P., & Zhang, J. (2020). Characterizing ecosystem functional type patterns based on subtractive fuzzy cluster means using Sentinel-2 time-series data. *Journal of Applied Remote Sensing*, 14(4), 048505–048505.

Limousin, J., Kempf, J., & Ourcival, J. (2025). ETC L2 ARCHIVE from puechabon, 2021–2024. *ICOS RI*. https://hdl.handle.net/11676/lH_jYf21wPDEj2thKE4S2k1h

Ma, X., Mahecha, M. D., Migliavacca, M., van der Plas, F., Benavides, R., Ratcliffe, S., Wirth, C., Kattge, J., Richter, R., Musavi, T., Baeten, L., Barnoaiea, I., Bohn, F. J., Bouriaud, O., Bussotti, F., Coppi, A., Domisch, T., Huth, A., Jaroszewicz, B., … Reichstein, M. (2019). Inferring plant functional diversity from space: The potential of Sentinel-2. *Remote Sensing of Environment*, *233*. 111368. https://doi.org/10.1016/j.rse.2019.111368

Mahecha, M. D., Bastos, A., Bohn, F. J., Eisenhauer, N., Feilhauer, H., Hartmann, H., Wirth, C., Hickler, T., Kalesse-Los, H., Migliavacca, M., Otto, F. E. L., Peng, J., Quaas, J., Tegen, I., Weigelt, A., & Wendisch, M. (2022). Biodiversity loss and climate extremes—study the feedbacks. *Nature*, *612*(7938), 30–32. https://doi.org/10.1038/d41586-022-04152-y

Mammarella, I., Aalto, J., Back, J., Kolari, P., Laakso, H., Levula, J., Matilainen, T., Pihlatie, M., Pumpanen, J., Ryhti, K., Taipale, R., & Vesala, T. (2025). ETC L2 ARCHIVE from hyytiala, 2018–2024. *ICOS RI*. https://hdl.handle.net/11676/oD2Pme94V4Cl6dmxyZDKuCeq

Manes, F., Vitale, M., Donato, E., Giannini, M., & Puppi, G. (2006). Different ability of three Mediterranean oak species to tolerate progressive water stress. *Photosynthetica*, *44*(3), 387–393. https://doi.org/10.1007/s11099-006-0040-7

Micol, R., Giulia, T., Rodolfo, G., Beatrice, S., Luigi, V., Jiawei, G., … Cinzia, P. (2024). Prisma images for the estimation of functional traits and biodiversity indices in mid-latitude forests, *In 2024 IEEE Mediterranean and Middle-East Geoscience and Remote Sensing Symposium (M2GARSS)* (pp. 352–355). IEEE.

Migliavacca, M., Musavi, T., Mahecha, M.D., Nelson, J. A., Knauer, J., Baldocchi, D. D., & Reichstein, M. (2021). The three major axes of terrestrial ecosystem function. Nature, 598(598), 468–472.

Moisen, G. G., Freeman, E. A., Blackard, J. A., Frescino, T. S., Zimmermann, N. E., & Jr, Edwards, T. C. (2006). Predicting tree species presence and basal area in Utah: A comparison of stochastic gradient boosting, generalized additive models, and tree-based methods. *Ecological modelling*, *199*(2), 176–187. https://doi.org/10.1016/j.ecolmodel.2006.05.021

Monteith, J. L. (1972). Solar radiation and productivity in tropical ecosystems. *Journal of Applied Ecology*, *9*(3), 747–766. https://doi.org/10.2307/2401901

Mouillot, D., Graham, N. A., Villéger, S., Mason, N. W., & Bellwood, D. R. (2013). A functional approach reveals community responses to disturbances. *Trends in ecology & evolution*, *28*(3), 167–177. https://doi.org/10.1016/j.tree.2012.10.004

Musavi, T., Mahecha, M. D., Migliavacca, M., Reichstein, M., van de Weg, M. J., van Bodegom, P. M., Kattge, J., Bahn, M., Wirth, C., Reich, P. B., & Schrodt, F. (2015). The imprint of plants on ecosystem functioning: A data-driven approach. *International Journal of Applied Earth Observation and Geoinformation*, *43*, 119–131. https://doi.org/10.1016/j.jag.2015.05.009

Musavi, T., Migliavacca, M., van de Weg, M. J., Kattge, J., Wohlfahrt, G., van Bodegom, P. M., Mahecha, M. D., Reichstein, M., Bahn, M., Carrara, A., Domingues, T. F., Gavazzi, M., Gianelle, D., Gimeno, C., Granier, A., Gruening, C., Havránková, K., Herbst, M., Hrynkiw, C., … Wirth, C. (2016). Potential and limitations of inferring ecosystem photosynthetic capacity from leaf functional traits. *Ecology and evolution*, *6*(20), 7352–7366. https://doi.org/10.1002/ece3.2479

Mutanga, O., & Kumar, L. (2019). Google earth engine applications. *Remote sensing*, *11*(5), 591. https://doi.org/10.3390/rs11050591

Nestola, E., Calfapietra, C., Emmerton, C. A., Wong, C. Y., Thayer, D. R., & Gamon, J. A. (2016). Monitoring grassland seasonal carbon dynamics, by integrating MODIS NDVI, proximal optical sampling, and eddy covariance measurements. *Remote Sensing*, *8*(3), 260. https://doi.org/10.3390/rs8030260

Nestola, E., Scartazza, A., Di Baccio, D., Castagna, A., Ranieri, A., Cammarano, M., Calfapietra, C., Mazzenga, F., & Matteucci, G. (2018). Are optical indices good proxies of seasonal changes in carbon fluxes and stress-related physiological status in a beech forest? *Science of the Total Environment*, *612*, 1030–1041. https://doi.org/10.1016/j.scitotenv.2017.08.167

Nilsson, M., Peichl, M., Marklund, P., Boschetti, F., De Simon, G., Holst, J., Smith, P., Kozii, N., Dignam, R., Larmanou, E., Lofvenius, P., Molder, M., Andersson, T., Linderson, M., & Lindgren, K. (2025). ETC L2 ARCHIVE from Degero, 2019–2024. *ICOS RI*. https://hdl.handle.net/11676/yRRAnKfmHZjaSbXHL9EL3JuK

Oke, T. R. (1987). *Boundary Layer Climates* (2nd ed.). Routledge. https://doi.org/10.4324/9780203407219

Pacheco-Labrador, J., El-Madany, T. S., Martin, M. P., Gonzalez-Cascon, R., Carrara, A., Moreno, G., … Migliavacca, M. (2020). Combining hyperspectral remote sensing and eddy covariance data streams for estimation of vegetation functional traits. *Biogeosciences Discussions*, *2020*, 1–38.

Pacheco-Labrador, J., El-Madany, T. S., Martín, M. P., Migliavacca, M., Rossini, M., Carrara, A., & Zarco-Tejada, P. J. (2017). Spatio-temporal relationships between optical information and carbon fluxes in a Mediterranean tree-grass ecosystem. *Remote Sensing*, *9*(6), 608. https://doi.org/10.3390/rs9060608

Parisi, F., D'Amico, G., Vangi, E., Chirici, G., Francini, S., Cocozza, C., Giannetti, F., Londi, G., Nocentini, S., Borghi, C., & Travaglini, D. (2024). Tree-related microhabitats and multi-taxon biodiversity quantification exploiting ALS data. *Forests*, *15*(4), 660. https://doi.org/10.3390/f15040660

Pastorello, G., Trotta, C., Canfora, E., Chu, H., Christianson, D., Cheah, Y., Poindexter, C., Chen, J., Elbashandy, A., Humphrey, M., Isaac, P., Polidori, D., Reichstein, M., Ribeca, A., van Ingen, C., Vuichard, N., Zhang, L., Amiro, B.,

Ammann, C., … Papale, D. (2020). The FLUXNET2015 dataset and the ONEFlux processing pipeline for eddy covariance data. *Scientific data*, *7*, 225. https://doi.org/10.1038/s41597-020-0534-3 ISSN: 2052-4463.
Pei, Y., Dong, J., Zhang, Y., Yuan, W., Doughty, R., Yang, J., Xiao, X., & Zhou, D. (2022). Evolution of light use efficiency models: Improvement, uncertainties, and implications. *Agricultural and Forest Meteorology*, *317*. 108905. https://doi.org/10.1016/j.agrformet.2022.108905
Peichl, M., Nilsson, M., Larmanou, E., Smith, P., Marklund, P., De Simon, G., Lofvenius, P., Dignam, R., Holst, J., Molder, M., Andersson, T., Boschetti, F., Kozii, N., Linderson, M., & Ottosson-Löfvenius, M. (2025). ETC L2 ARCHIVE from Svartberget, 2019–2024. *ICOS RI*. https://hdl.handle.net/11676/DLlJ-m63gJHSmiUipESYGuLd
Probst, P., Wright, M. N., & Boulesteix, A. L. (2019). Hyperparameters and tuning strategies for random forest. *Wiley Interdisciplinary Reviews: data mining and knowledge discovery*, *9*(3), e1301
Punalekar, S., Verhoef, A., Tatarenko, I. V., Van der Tol, C., Macdonald, D. M., Marchant, B., Gowing, D., Gerard, F., & White, K. (2016). Characterization of a highly biodiverse floodplain meadow using hyperspectral remote sensing within a plant functional trait framework. *Remote Sensing*, *8*(2), 112. https://doi.org/10.3390/rs8020112
Reichstein, M., Bahn, M., Mahecha, M. D., Kattge, J., & Baldocchi, D. D. (2014). Linking plant and ecosystem functional biogeography. *Proceedings of the National Academy of Sciences of the United States of America*, *111*(38), 13697–13702. https://doi.org/10.1073/pnas.1216065111
Savinelli, B., Panigada, C., Tagliabue, G., Vignali, L., Gentili, R., Fassnacht, F. E., Rossini, M., & Padoa-Schioppa, E. (2024). Monitoring functional traits of complex temperate forests using Sentinel-2 data during a severe drought period. *Science of The Total Environment*, *957*. 177428. https://doi.org/10.1016/j.scitotenv.2024.177428
Schmidt, J., Fassnacht, F. E., Lausch, A., & Schmidtlein, S. (2017). Assessing the functional signature of heathland landscapes via hyperspectral remote sensing. *Ecological Indicators*, *73*, 505–512. https://doi.org/10.1016/j.ecolind.2016.10.017
Schulze, E. D., Beck, E., Buchmann, N., Clemens, S., Müller-Hohenstein, K., Scherer-Lorenzen, M., … Scherer-Lorenzen, M. (2019). Interactions between plants, plant communities and the abiotic and biotic environment: With contributions from CF dormann and HM schaefer. *Plant ecology*, 689–741. https://doi.org/10.1007/978-3-662-56233-8_19
Stanhill, G. (1986). Water use efficiency. *Advances in agronomy*, *39*, 53–85. https://doi.org/10.1016/S0065-2113(08)60465-4
Tagliabue, G., Boschetti, M., Bramati, G., Candiani, G., Colombo, R., Nutini, F., Panigada, C., Pompilio, L., Rivera-Caicedo, J. P., Rossi, M., Rossini, M., & Verrelst, J. (2022). Hybrid retrieval of crop traits from multi-temporal PRISMA hyperspectral imagery. *ISPRS Journal of Photogrammetry and Remote Sensing*, *187*, 362–377. https://doi.org/10.1016/j.isprsjprs.2022.03.014
Thorpe, A. S., Barnett, D. T., Elmendorf, S. C., Hinckley, E. L. S., Hoekman, D., Jones, K. D., Thibault, K. M., LeVan, K. E., Meier, C. L., & Stanish, L. F. (2016). Introduction to the sampling designs of The National ecological observatory network terrestrial observation system. *Ecosphere*, *7*(12). e01627. https://doi.org/10.1002/ecs2.1627
Tramontana, G., Jung, M., Schwalm, C. R., Ichii, K., Camps-Valls, G., Ráduly, B., Merbold, L., Reichstein, M., Arain, M. A., Cescatti, A., Kiely, G., Serrano-Ortiz, P., Sickert, S., Wolf, S., & Papale, D. (2016). Predicting carbon dioxide and energy fluxes across global FLUXNET sites with regression algorithms. *Biogeosciences*, *13*(14), 4291–4313. https://doi.org/10.5194/bg-13-4291-2016
Tuittila, E., Kolari, P., Korrensalo, A., Laakso, H., Levula, J., Mammarella, I., Matilainen, T., Männistö, E., Taipale, R., & Vesala, T. (2025). ETC L2 ARCHIVE from Siikaneva, 2017–2024. *ICOS RI*. https://hdl.handle.net/11676/Q_v3L2WFG0jCq47RwLhJLnWV
Urban, O., Janouš, D., Acosta, M., Czerný, R., Markova, I., Navratil, M., Marek, M. V., MARKOVÁ, I., NAVRÁTIL, M., PAVELKA, M., POKORNÝ, R., ŠPRTOVÁ, M., ZHANG, R., ŠPUNDA, V., & GRACE, J. (2007). Ecophysiological controls over the net ecosystem exchange of mountain spruce stand. Comparison of the response in direct vs. Diffuse solar radiation. *Global Change Biology*, *13*(1), 157–168. https://doi.org/10.1111/j.1365-2486.2006.01265.x
Vaglio Laurin, G. (2025). Functional ecosystem properties estimated from satellite PRISMA and Sentinel-2 data in natural european sites [Data set]. *Zenodo*. https://doi.org/10.5281/zenodo.17762649
Vaglio Laurin, G., Sebastiani, A., Nardella, L., Calfapietra, C., Barbati, A., Ventura, B., & Papale, D. (2024). Linking hyperspectral PRISMA data with ecosystem functional properties at ICOS sites. *Remote Sensing for Agriculture, Ecosystems, and Hydrology XXVI*, *13191*, 170–175 SPIE.
Vaglio Laurin, G., Vittucci, C., Tramontana, G., Ferrazzoli, P., Guerriero, L., & Papale, D. (2020). Monitoring tropical forests under a functional perspective with satellite-based vegetation optical depth. *Global Change Biology*, *26*(6), 3402–3416. https://doi.org/10.1111/gcb.15072
Vekuri, H., Tuovinen, J. P., Kulmala, L., Papale, D., Kolari, P., Aurela, M., Lohila, A., Laurila, T., & Liski, J. (2023). A widely-used eddy covariance gap-filling method creates systematic bias in carbon balance estimates. *Scientific Reports*, *13*(1). 1720. https://doi.org/10.1038/s41598-023-28827-2
Vitale, D., Fratini, G., Bilancia, M., Nicolini, G., Sabbatini, S., & Papale, D. (2020). A robust data cleaning procedure for eddy covariance flux measurements. Biogeosciences, *17*, 1367–1391. https://doi.org/10.5194/bg-17-1367-2020 ISSN: 1726-4189.
Vogelmann, J. E., Rock, B. N., & Moss, D.M. (1993). Red edge spectral measurements from sugar maple leaves. *TitleREMOTE SENSING*, 14(8), 1563–1575.

Wright, I. J., Dong, N., Maire, V., Prentice, I. C., Westoby, M., Díaz, S., Wilf, P., Gallagher, R. V., Jacobs, B. F., Kooyman, R., Law, E. A., Leishman, M. R., Niinemets, Ü., Reich, P. B., Sack, L., Villar, R., & Wang, H. (2017). Global climatic drivers of leaf size. *Science*, *357*(6354), 917–921. https://doi.org/10.1126/science.aal4760

Wright, I. J., Reich, P. B., Westoby, M., Ackerly, D. D., Baruch, Z., Bongers, F., Villar, R., Cavender-Bares, J., Chapin, T., Cornelissen, J. H. C., Diemer, M., Flexas, J., Garnier, E., Groom, P. K., Gulias, J., Hikosaka, K., Lamont, B. B., Lee, T., Lusk, C., … Veneklaas, E. J. (2004). The worldwide leaf economics spectrum. *Nature*, *428*(6985), 821–827. https://doi.org/10.1038/nature02403

Wilson, B., Baldocchi, D. D., Aubinet, M., Berbigier, P., Bernhofer, C., Dolman, H., Wofsy, S., Falge, E., Field, C., Goldstein, A., Granier, A., Grelle, A., Halldor, T., Hollinger, D., Katul, G., Law, B. E., Lindroth, A., Meyers, T., Moncrieff, J., … Vesala, T. (2002). Energy partitioning between latent and sensible heat flux during the warm season at FLUXNET sites. *Water Resources Research*, *38*(12), 30–31. https://doi.org/10.1029/2001WR000989

Wu, C., Niu, Z., Tang, Q., & Huang, W. (2008). Estimating chlorophyll content from hyperspectral vegetation indices: Modeling and validation. *Agricultural and forest meteorology*, *148*(8-9), 1230–1241. https://doi.org/10.1016/j.agrformet.2008.03.005

Yoav, F., Robert Schapire, R., & Abe, N. (1999). A short introduction to boosting. *Journal-Japanese Society For Artificial Intelligence*, *14*, 771–780 1612.

Zabeo, C., Laurin, G. V., Tesfamariam, B. G., Giuliarelli, D., Valentini, R., & Barbati, A. (2024). A multi-source approach to mapping habitat diversity: Combination of multi-date multispectral satellite imagery and comparison with single-date hyperspectral results in a Mediterranean natural reserve. *Ecological Informatics*, *84*. 102867. https://doi.org/10.1016/j.ecoinf.2024.102867

Zhang, Y., Migliavacca, M., Penuelas, J., & Ju, W. (2021). Advances in hyperspectral remote sensing of vegetation traits and functions. *Remote Sensing of Environment*, *252*. 112121. https://doi.org/10.1016/j.rse.2020.112121

Zhang, W., Gu, X., Hong, L., Han, L., & Wang, L. (2023). Comprehensive review of machine learning in geotechnical reliability analysis: Algorithms, applications and further challenges. *Applied Soft Computing*, *136*. 110066. https://doi.org/10.1016/j.asoc.2023.110066

Zhao, Y., Sun, Y., Lu, X., Zhao, X., Yang, L., Sun, Z., & Bai, Y. (2021). Hyperspectral retrieval of leaf physiological traits and their links to ecosystem productivity in grassland monocultures. *Ecological Indicators*, *122*. 107267. https://doi.org/10.1016/j.ecolind.2020.107267